Wind and Structures, *Vol. 27, No. 2 (2018) 123-136*
DOI: https://doi.org/10.12989/was.2018.27.2.123

Topographic effects on tornado-like vortex

Zoheb Nasir and Girma T. Bitsuamlak*

Civil and Environmental Engineering/WindEEE Institute, Western University (formerly The University of Western Ontario), 1151 Richmond St, London, Canada

(Received April 4, 2018, Revised June 28, 2018, Accepted July 3, 2018)

Abstract. The effects of steep and shallow hills on a stationary tornado-like vortex with a swirl ratio of 0.4 are simulated and quantified as Fractional Speed Up Ratios (FSUR) at three different locations of the vortex with respect to the crests of the hills. Steady state Reynolds Averaged Naiver Stokes (RANS) equations closed using Reynolds Stress Turbulence model are used to simulate stationary tornadoes. The tornado wind field obtained from the numerical simulations is first validated with previous experimental and numerical studies by comparing radial and tangential velocities, and ground static pressure. A modified fractional speed-up ratio (FSUR) evaluation technique, appropriate to the complexity of the tornadic flow, is then developed. The effects of the hill on the radial, tangential and vertical flow components are assessed. It is observed that the effect of the hill on the radial and vertical component of the flow is more pronounced, compared to the tangential component. Besides, the presence of the hill is also seen to relocate the center of tornadic flow. New FSUR values are produced for shallow and steep hills.

Keywords: tornado; topography; speed-up; Fractional Speed Up Ratio (FSUR); numerical simulation

1. Introduction

Previous studies have used both laboratory and numerical simulations to analyze tornado-like flow and its interaction with structures. Ward (1972) built a tornado vortex chamber (TVC) with geometric and dynamic similarity to a real tornado. Later, Davies Jones (1973) conducted a parametric study to investigate the dependency of core radius on various parameters like swirl ratio, inflow depth, updraft radius and reinterpreted Ward (1972) by concluding that the volume flow rate, and not the radial momentum flux, is an important parameter in sustaining such vortices. Church *et al*. (1979) used a Ward type tornado simulator to identify the important transition points in a tornadic flow structure and concluded that the vortex flow structure is independent of radial Reynolds number above a threshold. Mitsuta and Monji (1984) used laboratory scaled model to simulate one and two-celled tornadoes and reported that the maximum horizontal velocity occurs near the ground surface and the height of this maximum velocity is insensitive to the swirl ratio. Diamond and Wilkins (1984) modified the original design by Ward (1972) by installing a movable ground plate to facilitate relative motion between the ground and vortex to study the influence of translation and concluded that translation causes a local increase in the swirl ratio and an increase in the size of the core radius compared to a stationary vortex. Haan *et al*. (2008, 2010) used the Iowa State University (ISU) Tornado Simulator to simulate tornadoes of different swirl ratios, they also compared peak load from the impact of tornadic flow on a model low-rise building with those prescribed by the ASCE 7-05 for straight wind over open terrain. Matsui and Tamura (2009) simulated tornadoes of different intensities for different floor roughness conditions and found that floor roughness is more influential for low swirl ratios compared to higher swirl ratios. Zhang and Sarkar (2009) used the ISU Tornado Simulator to analyze the flow structure near the ground and found that the tangential velocity is the dominant component of flow and its peak value is three times higher than radial velocity component. Tari *et al.* (2010) also simulated tornadoes of different swirl ratios and found the radial and tangential velocity components of flow as well as the core radius increase with the higher swirl ratio values. Refan *et al*. (2013) used Model WindEEE Dome at the University of Western Ontario to simulate tornadoes of different swirl ratio and compared the location of the maximum tangential velocity point with real tornadoes to develop consistent geometric scaling approach for tornadic flows.

In parallel with these experimental efforts, several numerical studies have also been conducted to study tornado-like flow field. Harlow and Stein (1974) simulated tornadoes of different intensities and analyzed various flow related parameters. Rotunno (1977, 1979) numerically modeled Ward's tornado simulator and analyzed the flow structure for different swirl ratio values. Church et al. (1993) reported that as swirl ratio increases, the altitude of vortex breakdown decreases until swirl ratio, S = 0.45. Nolan and Ferrell (1999) proposed that vortex Reynolds number controls the flow structure and maximum wind speed of the tornado flow. Lewellen and Lewellen (1997, 2007) numerically simulated a three-dimensional tornado and analysed the flow structure near the ground. Kuai *et al.* (2008) replicated the ISU Tornado Simulator numerically and compared their results with the laboratory model.

*Corresponding author, Professor
E-mail: gbitsuam@uwo.ca

Copyright © 2018 Techno-Press, Ltd.

ISSN: 1226-6116 (Print), 1598-6225 (Online)

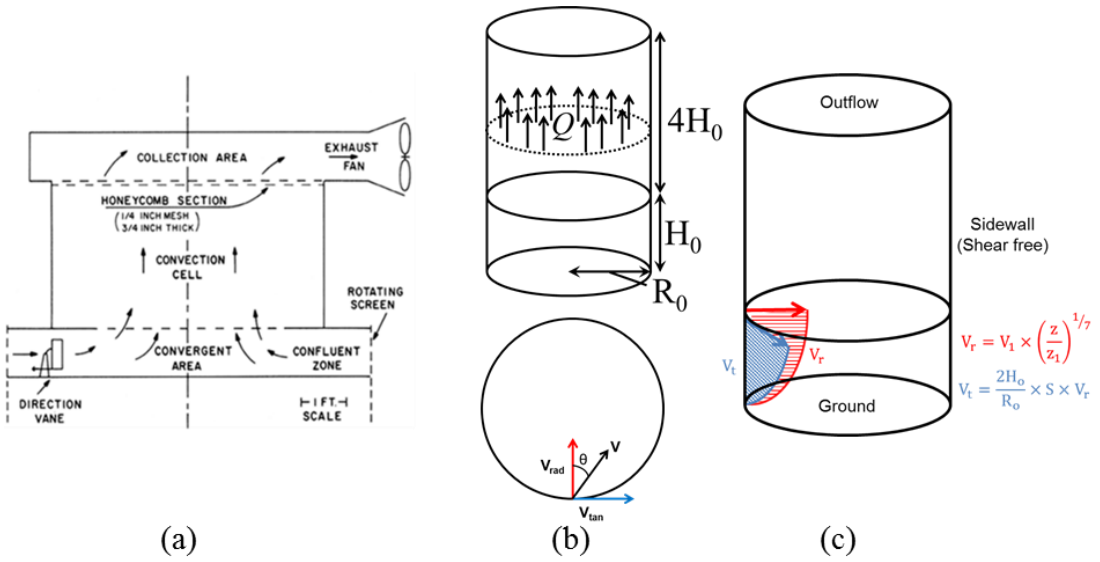

Fig. 1 (a) Laboratory, (b) modified numerical model of Ward's tornado vortex chamber, and (c) boundary conditions

Hangan and Kim (2008) used their simulation to analyse the dependency of flow dynamics on swirl ratio and its relation with the Fujita scale. Ishihara *et al*. (2011) simulated tornadic flow using large eddy simulation technique for two swirl ratios which represented one and two-celled tornadoes and reported that for one-celled type vortex peak vertical velocity occurs at the center, while for two-celled vortex the peak occurs near the radius of the maximum tangential wind. Hangan and Natarajan (2012) used large eddy simulations to analyze the impact of ground surface roughness and translation. They reported that translation reduces the maximum mean tangential velocity for low swirl ratio, however for high swirl ratio it increased it slightly. Ground roughness was also reported to decrease the mean tangential velocity at all swirl ratios.

Although a number of studies exist on topography effect on synoptic flow (Bitsuamlak *et al.* 2004, 2006, 2007, Abdi and Bitsuamlak 2014 and many others), studies on topographic effect on non-synoptic with the objective of evaluating speed up are very limited. More recently, some studies have considered the effect of topography over the path of tornado. For example, Karstens *et al.* (2012) simulated an experimental model in ISU tornado simulator to determine the effect of topography and obtained that tornado path deviated from its original direction as it climbs up and down a hill. Lewellen (2012), used immersed boundary method and large eddy simulation (LES) to simulate tornadoes of different intensities over different topographical changes in 3-dimensional domains. They analyzed the change in tornado path, structure and intensity over different topographical changes. The main objective of these studies is to analyze the change in flow structure in the presence of topographical changes. The present study focuses in generating flow speed-up parameters useful for engineering design. Due to the complexity of the problem and the time required to conduct unsteady simulations, the scope of the present study is limited to a steady state numerical approach.

2. Methodology

2.1 Numerical model

For the present study, a numerical model that utilizes the Purdue tornado simulator to obtain the geometric dimensions of the computational domain is used (see Fig. 1(a)). The Purdue tornado simulator is cylindrical in shape, where air enters the simulator from the bottom part near the ground. Guide vanes are installed at the inlet to impart the desired angle in the inflow. Once the swirling flow enters inside the simulator through the confluent region, it reroutes vertically upward in the convection region. To facilitate the vertical movement of the flow, an exhaust fan is installed at the outlet to pump the air out from the simulator. While keeping similar principle of operation, some modification is made to the simplified cylindrical numerical model (see Fig. 1(b)). In this paper, the numerical model is called "simplified" because it only replicates the flow-field in the convergent zone of the physical simulator; the region of flow-field that is of interest for engineering applications. In the numerical model, the lower peripheral surface of the cylindrical domain is treated as the inflow, where radial and tangential velocity components of the flow are specified to mimic the effect of guide vanes that provide swirl to the flow in the physical simulator. A "shear free" or "slip wall" boundary condition is specified at the sidewall and the outlet, which is kept "far away" from the inflow, is treated as "pressure outflow". The dimensions of the original laboratory simulator are scaled up following the procedure proposed in Refan *et al*. (2013) to obtain the dimensions of the "simplified" computational domain for numerical simulations.

The computational domain used for present numerical tornado simulation has the following dimensions, H_0=1730 m and R_0= 1700 m (see Figs. 1(c) and 2(a)). The ground surface is altered using a sinusoidal function (see Fig. 2(b)) to create the hills. Two different types of hills, steep and

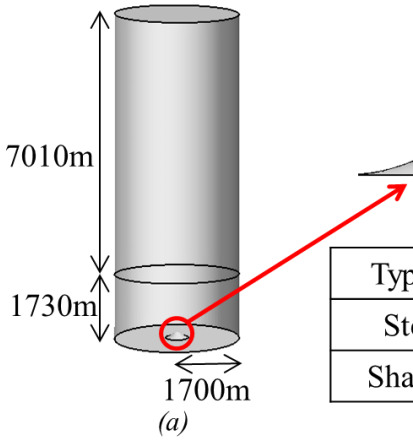

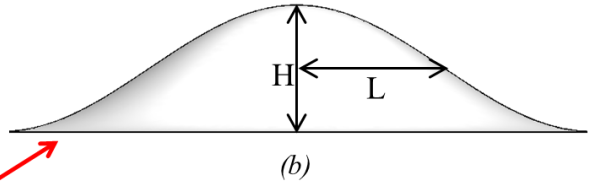

Type of hill	H	L	H/L
Steep hill	160	160	1
Shallow hill	160	320	0.5

(c)

Location	Tornado center
1	At hill crest
2	At half-height of the hill
3	At foot of the hill

Fig. 2 Dimensions for (a) full computational domain and (b), (c) hills

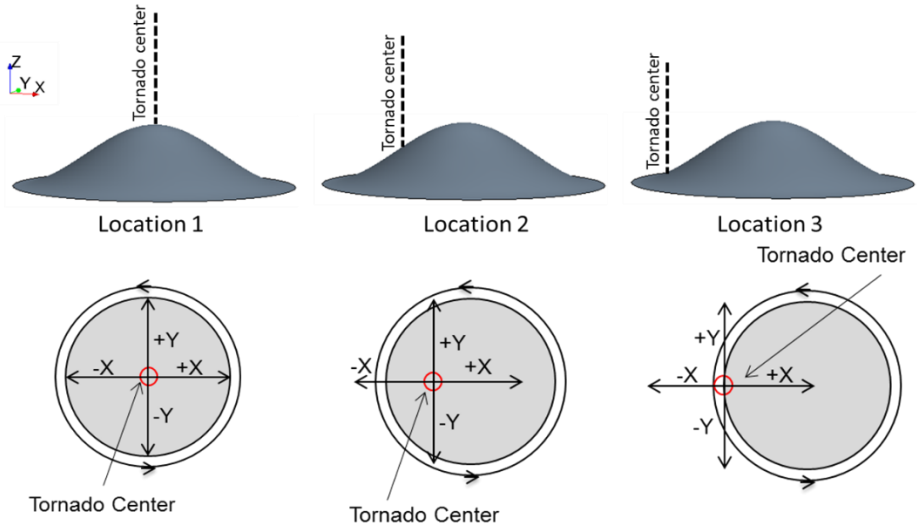

Fig. 3 Location of tornado with respect to the crest of the hill

shallow, respectively are considered (see Figs 2b and 2c). Three locations of a stationary tornado center with respect to the crest of the hill are considered by moving the tornado center along the *X*-axis (see Fig. 3). More specifically the three locations represent cases when the tornado center coincides with the crest of the hill (Location 1), the half-height of the hill (Location 2) and the foot of the hill (Location 3), respectively. A commercial Computational Fluid Dynamics (CFD) solver called STAR-CCM+ is used to carry out all the simulations.

The Reynolds Averaged Navier-Stokes (RANS) equations are of similar form as Navier-Stokes (NS) equations if instantaneous quantities are replaced by mean quantities, except RANS equations have additional unknown terms called Reynolds stresses. Various turbulence models under the RANS framework are deployed to tackle these additional unknown terms (or the Reynolds stresses) and close the system of governing equations. While the eddy viscosity models like $k-\varepsilon$ and $k-\omega$ use Boussinesq assumption to relate Reynolds stresses to mean flow properties, Reynolds Stress Model (RSM) solves six additional transport equations (one for each Reynolds stress) and therefore captures more physics. Reynolds Averaged Navier-Stokes (RANS) equations are used together with the Reynolds Stress Model (RSM) for steady state simulations in the present study. RSM

turbulence model is chosen over eddy viscosity models because of its better accuracy to model rotating flows. The eddy models are based on the Boussinesq assumption which postulates that, the Reynolds stress tensor must be proportional to the strain rate tensor. However, for complex flows, such as tornadic flow, this particular assumption does not work because of the curvature effects. The Reynolds Stress Model (RSM) for turbulence closure in the RANS framework is the most complete physical representation of the flow. The transport equation for Reynolds stress can be obtained by multiplying the NS with fluctuations and then averaging as shown

$$\overline{u_i NS(U_j + u_j) + u_j NS(U_i + u_i)} = 0$$

$$\frac{D(\overline{u_i u_j})}{Dt} = -\frac{\partial}{\partial x_l}\left[-\overline{u_i u_j u_l} - \frac{p}{\rho}\left(\delta_{jl}u_i + \delta_{il}u_j\right)\right] + \nu\frac{\partial \overline{u_i u_j}}{\partial x_l}$$

$$-\left(\overline{u_i u_l}\frac{\partial U_j}{\partial x_l} + \overline{u_j u_l}\frac{\partial U_i}{\partial x_l}\right) + \left(2\nu\overline{\frac{\partial u_i}{\partial x_l}\frac{\partial u_j}{\partial x_l}}\right) + \frac{p}{\rho}\left(\frac{\partial u_i}{\partial x_l} + \frac{\partial u_j}{\partial x_l}\right)$$

Here, δ is the Kronecker delta function, U is the mean velocity, u is the fluctuating velocity, p is the pressure, ν is the kinematic viscosity and ρ is the density. The first, second, third, fourth and fifth terms on the right-hand side of the above equation are the turbulent diffusion, molecular diffusion, production, dissipation and pressure-strain interaction terms, respectively. It can be seen that this equation has additional third order moment term ($\overline{u_i u_j u_l}$). The transport equation for third order moment term would give rise to fourth order moment term and so on. This essentially leads us to the problem of turbulence closure. While solving the transport equations for subsequently higher order moments would capture more physics, it would also make the computation very expensive. Therefore, RSM works out a trade off by modelling the five terms in the transport equations of the first order moments with the help of semi empirical relations, certain details of which can be found in Launder *et al.* (1975).

As previously mentioned, two velocity components (radial and tangential) are provided in the inflow to produce a swirling flow field. The equation for the radial and tangential velocity components are as follows

$$V_r = V_1 \times \left(\frac{z}{z_1}\right)^{1/7} \quad (1\text{-}1)$$

$$V_t = \frac{2H_o}{R_o} \times S \times V_r \quad (1\text{-}2)$$

Here, V_r and V_t are the radial and tangential component of velocity at 'z' height from ground surface respectively. 'S' is the swirl ratio which is a measure of the strength of circulation relative to convection in the flow-field. $S = \frac{v_t}{v_r 2a}$; v_t and v_r are the two velocity vectors at the inlet and 'a' is the aspect ratio; $a = \frac{Ho}{Ro}$ (See Fig. 1(b)). H_o and R_o are the inlet height and radius of inlet respectively. Reference velocity, V_1 and height, z_1 are chosen at 10m/s and 106m are chosen respectively based on the actual data obtained from the tornadic event that took place in Happy, Texas in 2007.

2.2 Discretization and grid independence

Polyhedral cells are used to discretize the computational domain and the base mesh size is kept comparatively coarse because of the large domain size. The mesh size near the ground and around the hills are kept very fine (wall *Y-plus* < 2) to capture the sharp velocity changes near the wall region (see Figs. 4(a)-4(c))

Grid independence test is carried out for a single case of swirl ratio 0.4 and with the topography located at the core center. Two different grid densities are used. The coarse grid (G1) has a total number of 1.5 million cells while the fine grid (G2) has 4 million cells. The maximum error for measuring maximum speed-up at the crest of the steep hill was found to be under 2%, indicating the simulations were independent of the grid size. Further, the characteristic ground static pressure profiles were also compared for the two grid resolutions and the solution was found to be independent of grid (Fig. 4(d)). The coarser of the two grids was adopted for the remaining study.

2.3 Fractional Speed-up Ratio (FSUR) definition

Fractional Speed-Up Ratio (FSUR) is typically used to represent the flow change due to topography (Bitsuamlak 2004). For synoptic flow-field, FSUR is defined as $U(z)/U_o(z)$, where $U(z)$ is the velocity at height 'z' above the hill surface and $U_o(z)$ is the upstream velocity at the same height from the flat ground (see Fig. 5).

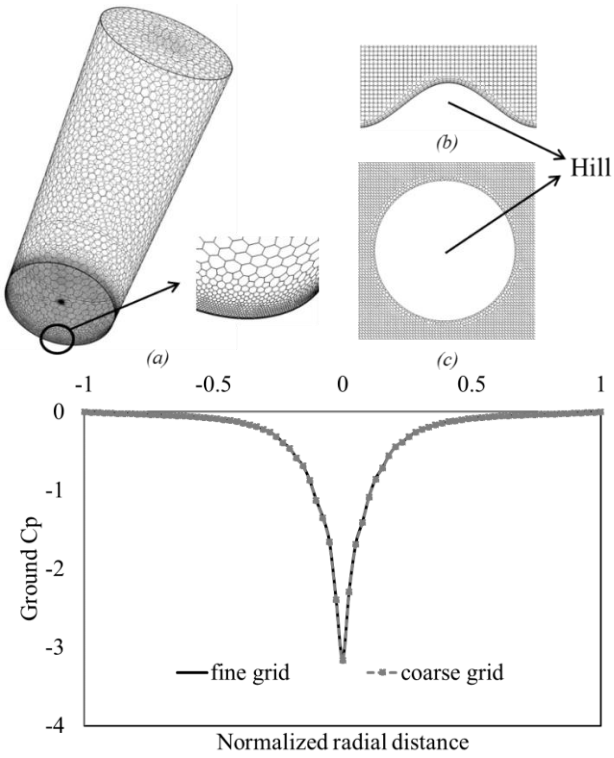

Fig. 4 Mesh distribution - finer mesh close to (a) the ground around (b), (c) hill and (d) grid independence

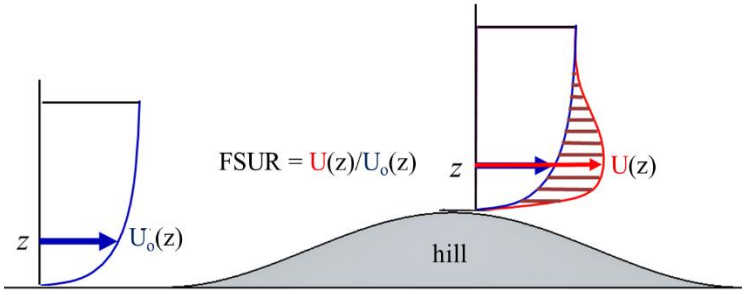

Fig. 5 FSUR calculation for synoptic flow

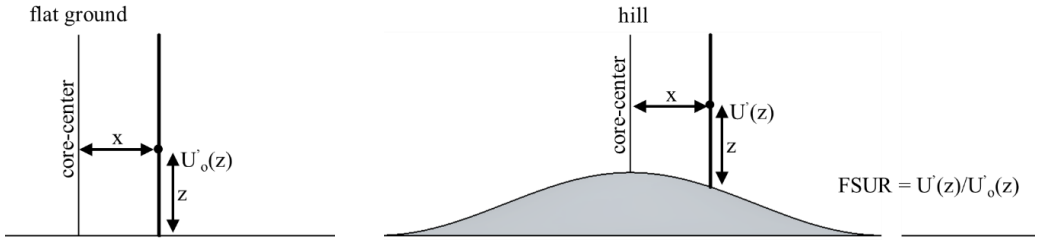

Fig. 6 FSUR calculation for tornadic flow over a hill

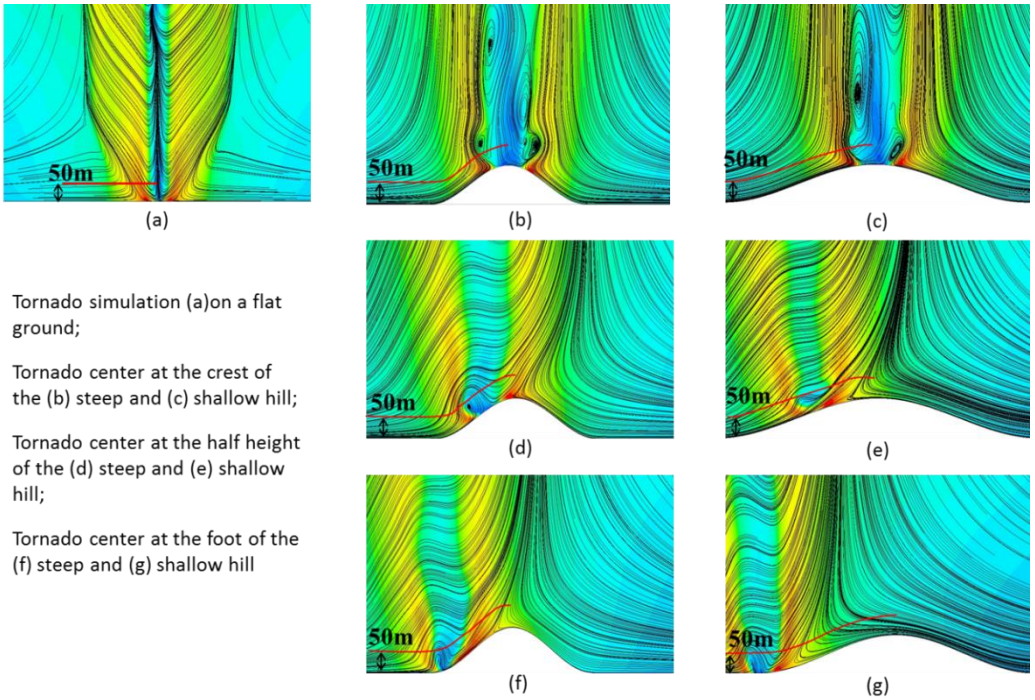

Fig. 7 Visual comparison of tornado flow-structure for various cases using streamlines and velocity distribution in the flow-field

Unlike synoptic flow, tornado has a complex three dimensional flow structure which consists of tangential, radial and vertical velocity components. As a result, a new FSUR calculation method is proposed in a slightly different manner. For tornado, FSUR is obtained by *U'(z)/U$_o$'(z)*, where *U'(z)* is the net velocity at height '*z*' above the hill surface at a given location in the tornado flow-field and *U$_o$'(z)* is the net velocity at the same height at the same location inside the tornado but in the absence of the hill (see Figs. 6 and 7).

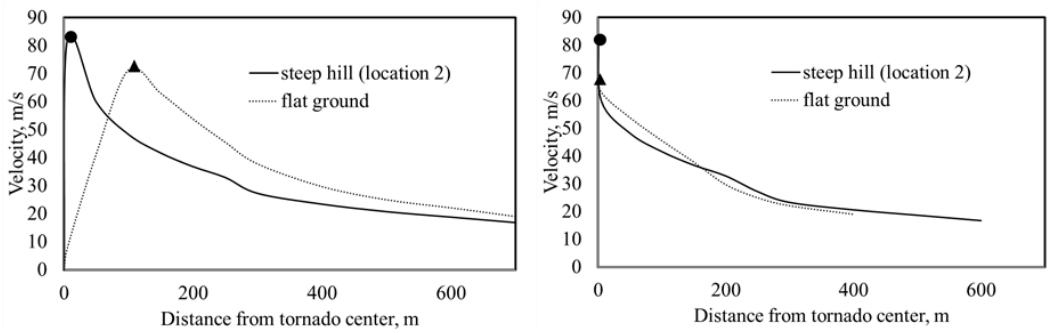

Fig. 8 Velocity field distribution with and without the presence of the hill (a) as is case (b) max value shifted to the origin

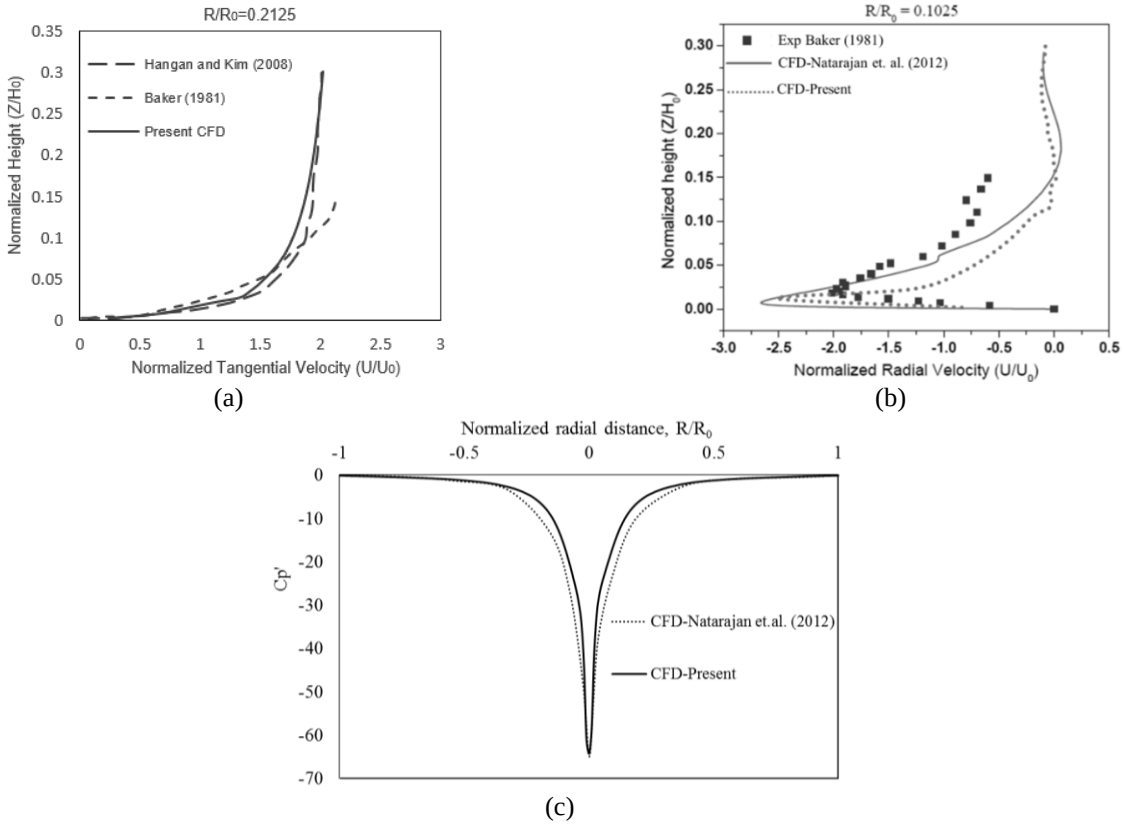

Fig. 9 Comparison of (a) tangential velocity along R/R0 = 0.2125 for S = 0.28, (b) radial velocity along R/R0 = 0.1025 for S = 0.28 and (c) ground Cp' for S = 0.40

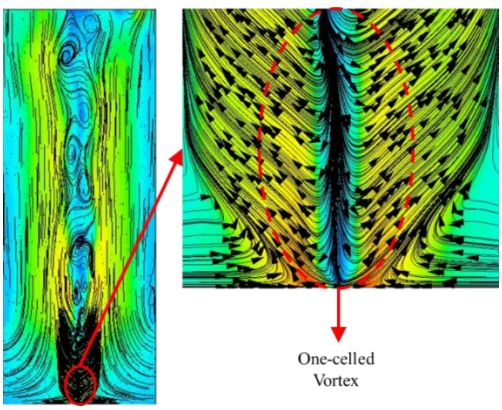

Fig. 10 Vertical flow structure (vector filed) of tornado-like vortex having swirl ratio 0.4 (one-celled vortex)

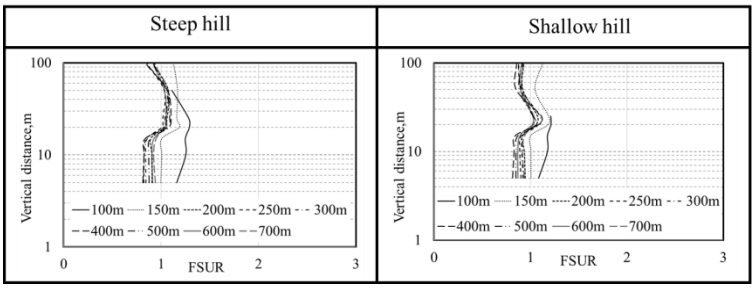

Fig. 11 Comparison of FSUR for tornado at Location 1 along X-axis

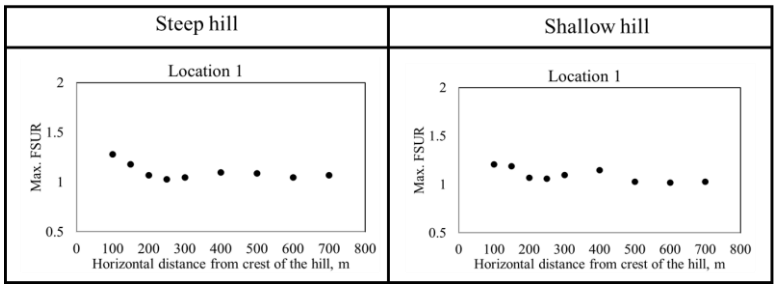

Fig. 12 Comparison of Max. FSUR along X-axis

A preliminary analysis showed that disruption in flow symmetry caused by the presence of hill demanded extra caution while evaluating FSUR, which has been illustrated in the following section. Fig. 7 shows two horizontal line-probes placed at same height (50m from the ground surface) for tornado on flat ground and on the hill. In Fig. 7(b), downward vortex flow at the center of the tornado touches at the half height of the hill. Due to this, the symmetry of the flow-field around the center of the tornado is disrupted, compared to the flow-field on flat terrain (Fig. 7(a)). Figs. 7(b)-7(g) shows the streamlines and velocity distribution inside the flow field for various locations of the vortex (with respect to hill crest) for both, steep and shallow hills. As shown in Fig. 8, it is seen that the overall flow distribution follows Rankine type distribution, which is common with the rotating flows. However, in the presence of the hill, the location of the maximum velocity shifts closer to the center of the tornado (i.e., the origin '0' in the figure). Keeping the location same, the velocity for the other case (tornado on a flat ground) is very small. As a result, evaluating FSUR using current methodology results in an unreasonably high value due to "division by a small number", which is not representative of reality. Hence defining the FSUR by direct comparison of symmetric and asymmetric tornado-like flow-fields may not be the best approach. To avoid this, a new approach is developed where the velocity profile for flat ground is intentionally off-set from its original position (see Fig. 8(a)) while evaluating the FSUR ratio, so that the location of the maximum velocity for both the cases coincides as shown in Fig. 8(b). The evaluation of the modified FSUR value starts from this maximum velocity location and continues along the line-probes. In this manner, more representative FSUR values are generated for tornadic flows. This procedure has been adopted to evaluate FSUR in the rest of the study.

3. Results and discussion

3.1 Tornado field validation

As initial validation of the numerically generated tornado flow-field in the present study, a vortex with a swirl ratio S =0.28 is simulated to compare the tangential and radial velocity profiles with experimental results of Baker (1981) and numerical results of Hangan and Kim (2008) and Natarajan *et al.* (2012). Comparison of vertical variation of tangential velocity obtained from present CFD simulations with experimental results of Baker (1981) and CFD results of Hangan and Kim (2008) at R/R0=0.2125 for a swirl ratio of 0.28 is shown in Fig. 9(a). It should be noted that the vertical distance has been normalized with inlet depth (H0) and the tangential velocity has been normalized by average inflow radial velocity, in compliance with the two previous studies used for comparison here. Similarly, the vertical variation of the normalized radial velocity at R/R0=0.1025 is plotted and compared with Baker (1981) and Natarajan *et al.* (2012) in Fig. 9(b) Both comparisons (tangential and radial velocities) show a good match with present CFD simulations (see Figs. 9(a) and 9(b)).

As previously mentioned, a tornado-like vortex with a swirl ratio S = 0.4, which is presumably a single celled vortex (see Fig. 10), is simulated to analyze topographic effects in this study. Therefore, in addition, the ground pressure coefficient distribution ($C_P{}'$) for this swirl ratio is also compared with numerical work of Natarajan *et al.* (2012) (See Fig. 9(c)). The ground pressure coefficient is computed using the following equation

$$C_P' = \frac{P - P_0}{0.5\rho U_0^2} \tag{1-3}$$

Where P is the pressure of the surface, P_0 is the far field

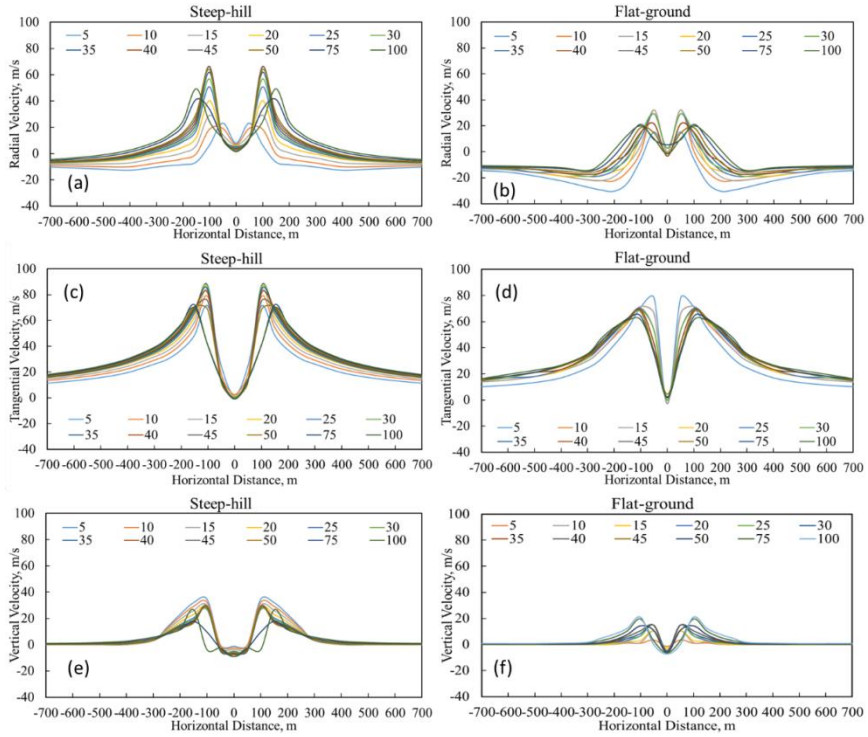

Fig. 13 Comparison of different velocity components of tornadic flow, for tornado at Location 1 along X-direction

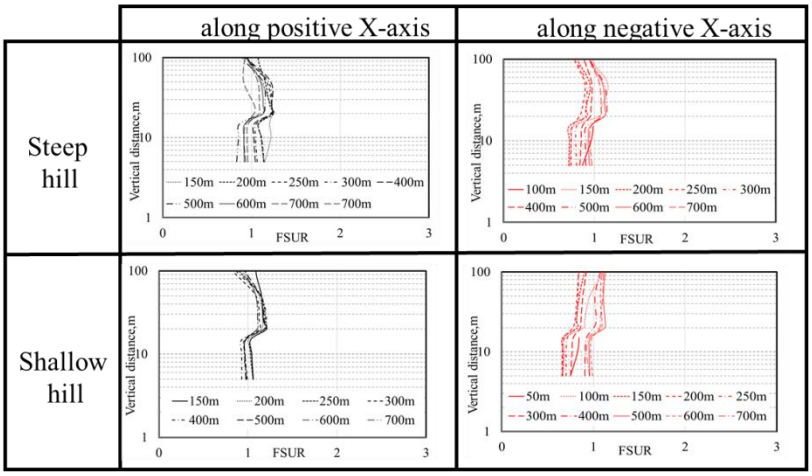

Fig. 14 Comparison of FSUR for tornado at Location 2 along X-axis

static pressure at the ground (located at the radius of updraft, which in the present numerical arrangement is the inlet), ρ is the density of air and U_0 is the reference velocity, which is average radial velocity at the inlet. Fig. 10(c) shows a good agreement between Natarajan *et al.* (2012) and the current simulation.

3.2 FSUR comparisons

The FSUR values for tornado at Location 1 are shown in Fig. 11. Irrespective of the horizontal distance along the *X*-direction from the tornado center, the maximum FSUR occurs at around 20 m high from the ground for both the steep and shallow hills (see Fig. 11). From Fig. 12, it can also be seen that the maximum FSUR is higher near the crest of the hill, irrespective of the type of the hill and then speed-up dies out for locations at the foot of the hill for both steep and shallow hill cases.

Considering the complexity of tornado-like flow-field, the variations in each velocity component are analyzed to better understand the nature of FSUR.

For the radial component of the flow, positive value indicates radially outward flow and negative value indicates radially inward flow. For the flat ground case, the inward radial flow becomes stronger as it moves closer to the core region and then near the vicinity of the core it changes its direction upward (Fig. 13(b)). However, inside the core region due to the vortex break down, downward

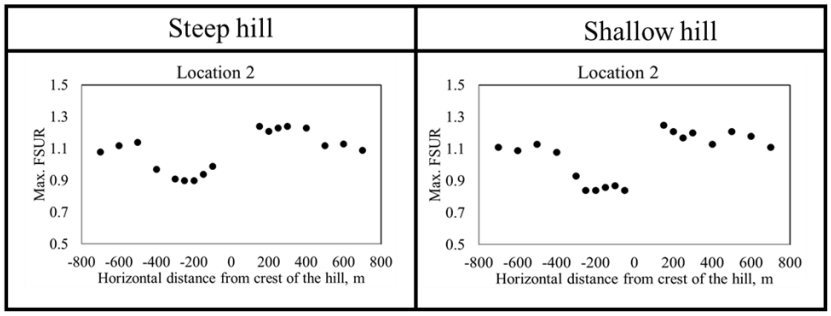

Fig. 15 Comparison of FSUR and Max. FSUR at Location 2 (along X-axis)

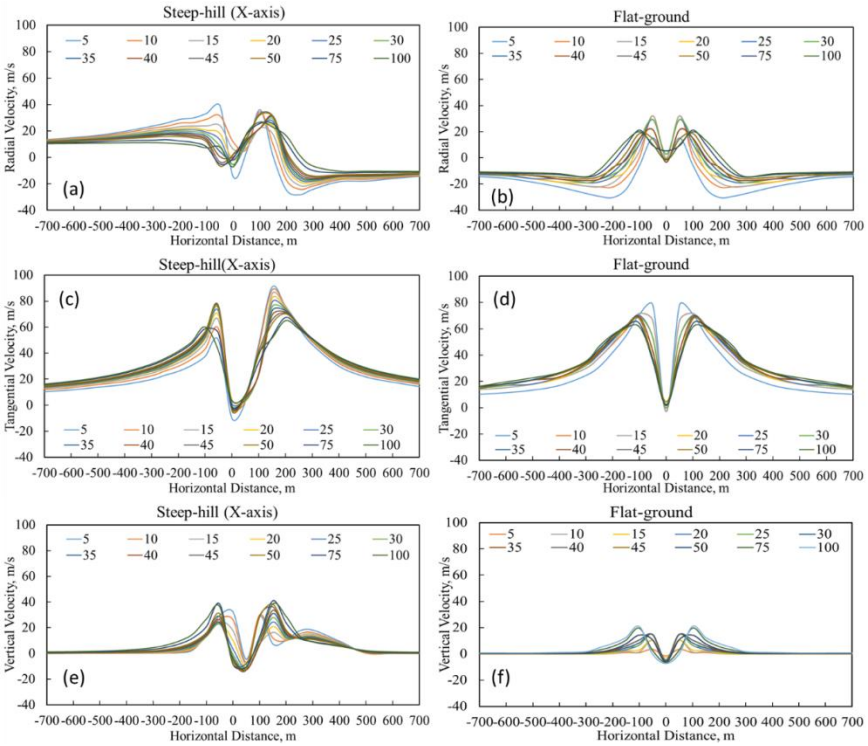

Fig. 16 Comparison of different velocity components of tornadic flow at Location 2 along X-axis

flow closer to the ground changes its direction radially outward from the center. In the presence of the hill, this radially outward flow becomes more prominent as slope of the hill enhances the transformation of vertical downward flow to radially outward flow (Fig. 13(a)). For the tangential direction of flow, the presence of the hill does not affect it significantly (Figs. 13(c) and 13(d)). However, for vertical direction of flow, the presence of the hill, enhance both upward and downward direction of flow (Figs. 13 (e) and 13(f)).

Likewise, the FSUR values for tornado at Location 2 are shown in Fig. 14. Overall, the speed-ups are higher along positive *X*-axis (which is the uphill zone) compared to negative *X*-axis (which is the downhill slope). Fig. 15 shows the maximum FSUR distribution. Generally, the speed up values are in comparable order of magnitude with those seen in synoptic wind flows.

The variations of each velocity component for tornado Location 2 are provided in Fig. 16. Along the negative *X*-axis, it is observed that the direction of flow is radially outward (see Fig. 16). This is due to the inclined surface of the hill, which actually disrupts the circular distribution of the flow. In addition, tornado center is also observed to relocate (see Fig. 17).

The FSUR distribution for tornado at Location 3 is similar to the one at Location 2, except in this case, the difference in maximum FSUR distribution along uphill (positive *X*-axis) and downhill (negative *X*-axis) slope is less when compared with tornado at Location 2 (Fig. 18).

The FSUR values are higher along the positive *Y*-axis compared to the negative *Y*-axis. Again, this can be determined by analyzing different components of flow. From the radial velocity distribution, it can be observed that the along negative *Y*-axis radial flow is outward, however along positive Y-axis the flow is inward (Fig. 20).

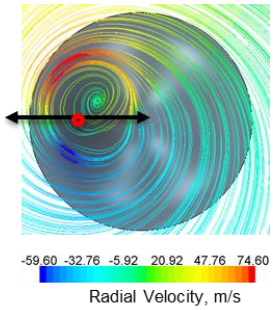

Fig. 17 Tornado center shift at Location 2

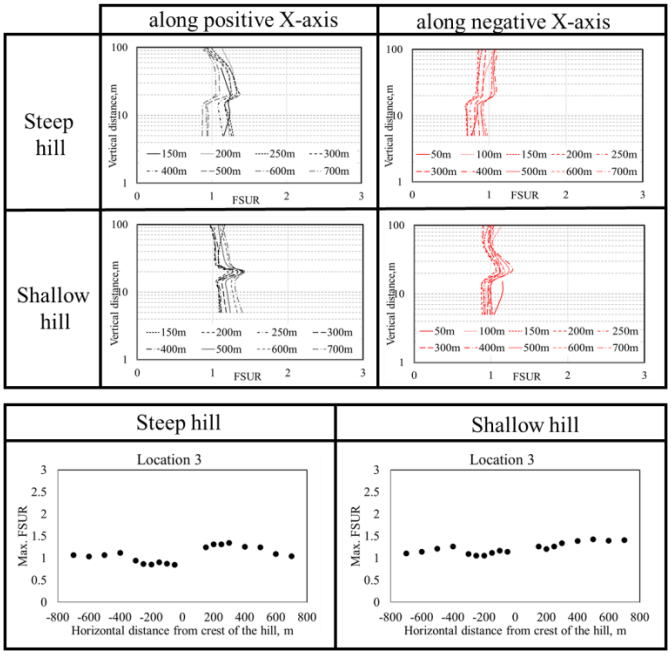

Fig. 18 Comparison of FSUR and Max. FSUR for tornado at Location 3 along X-axis

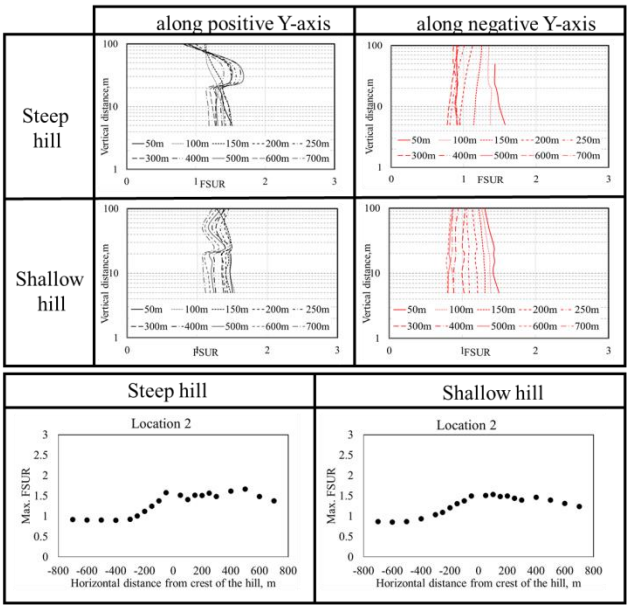

Fig. 19 Comparison of FSUR and Max. FSUR at tornado Location 2 along Y-axis

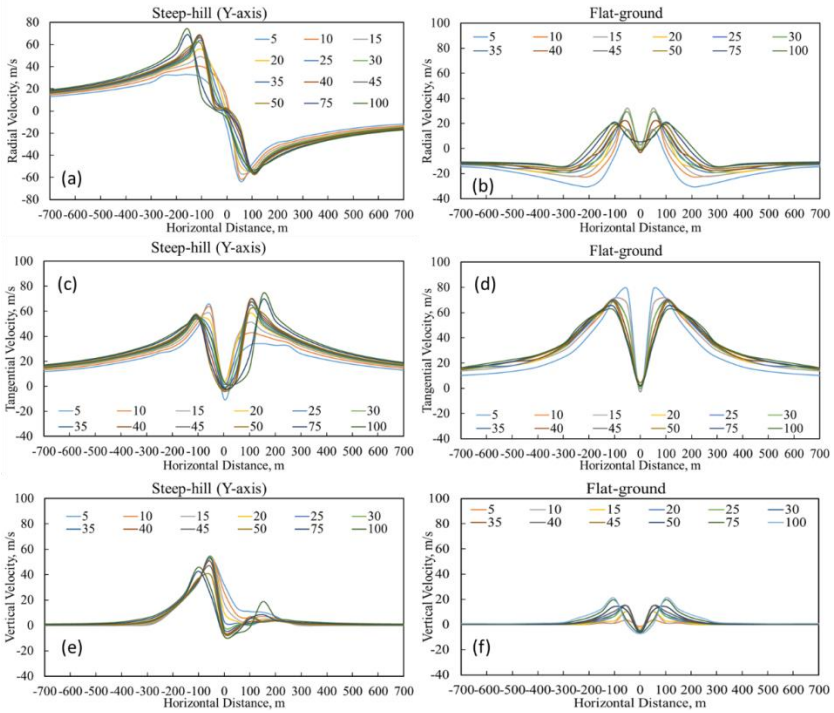

Fig. 20 Comparison of different components of tornadic flow for tornado at Location 2 along Y-axis

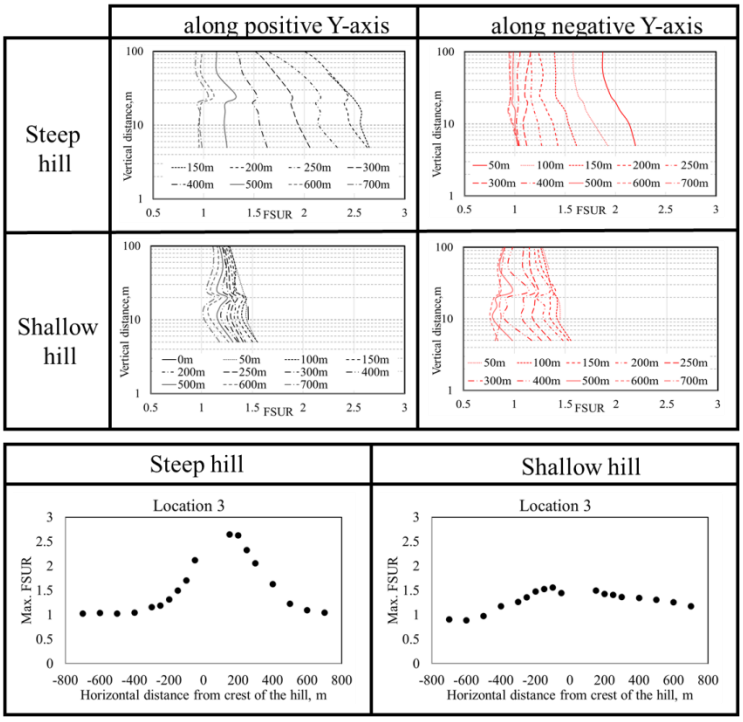

Fig. 21 Comparison of FSUR and Max. FSUR for tornado at Location 3 along Y-axis

Similar FSUR distribution is also observed for tornado at Location 3 (along *Y*-axis). However, for steep hill, speed-up increases by around 2.5 times near the tornado center. This is due to the increase in upward velocity (see Fig. 21). Here upward velocity increases due to the presence of the downhill slope which is concave in shape and enhances the updraft strength (Fig. 22).

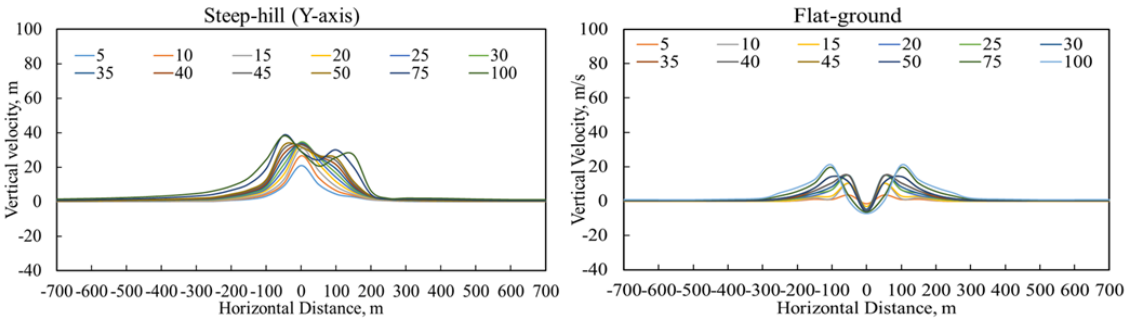

Fig. 22 Vertical components of flow distribution for tornado at Location 3 along Y-axis

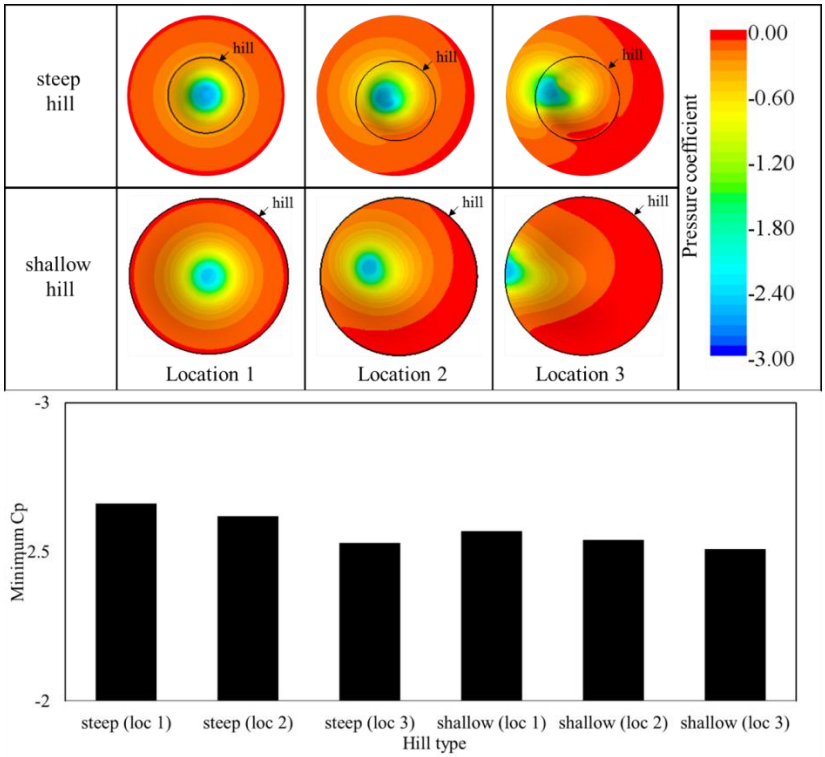

Fig. 23 Ground Cp comparison between steep and shallow hills

3.3 Comparison of Cp at the ground level

Pressure coefficient, *Cp*, on the ground is obtained using equation 1-3. In this case, the reference velocity is used as the maximum tangential velocity at the crest height of the hill in the absence of the hill. In Fig. 23, for all the cases the plots are cropped to the size of the radius of the shallow hill to facilitate the visual comparison. For all the cases, the pressure distribution is similar where maximum suction (minimum *Cp*) occurs at the center of the tornado and decreases as it moves away from the center (see Fig. 23). This indicates, the slope of the hill affects the overall pressure distribution on the ground slightly as shown in Fig.23.

4. Conclusions

Based on the present numerical arrangements and selected flow structure of the simulated vortex, following conclusions can be made:

- A pragmatic FSUR evaluation method has been developed for tornado-like flow field and FSUR values generated for shallow and steep hills.
- In the presence of hill (steep or shallow), the location of maximum velocity shifts much closer to the tornado center, irrespective of the location of tornado (with respect to the crest of the hill).
- Irrespective of the location of the tornado with respect to the hill, speed-up occurs for all the cases.
- When the tornado center coincides with the crest of the hill, the region of downward flow expands near the hill surface which increases the radial component of the flow.

- As tornado center coincides with the inclined surface of the hill, the downward flow becomes tilted which in turn disrupts the symmetric distribution of radial and vertical distribution of the flow.
- The slope of the hill does not affect the overall pressure distribution on the ground significantly. Only the location of maximum suction changes depending upon the location of tornado center.
- The FSUR results obtained in the present study are applicable only to small topographical features, as large mountains and valleys could disrupt fully the tornado structure.

Acknowledgements

The authors would like to acknowledge the financial support from the National Research Council of Canada (NSERC), Ontario Center of Excellence, Hydro One, and Canada Research Chair (for the second author). The authors are grateful for access to SHARCNET (a high-performance computing facility) and support received from their excellent technical support team.

References

Abdi, D. and Bitsuamlak, G.T. (2014), "Wind flow simulations on idealized and real complex terrain using various turbulence models", *Adv. Eng. Softw*., **75**, 30-41.

Baker, D. E., 1981. Boundary layers in laminar vortex flows. Ph.D. thesis, Purdue University.

Bitsuamlak, G.T., Stathopoulos, T. and Bédard, C. (2004), "Numerical evaluation of turbulent flows over complex terrains: A review", *J. Aerosp. Eng*., **17**(4), 135-145.

Bitsuamlak, G.T., Stathopoulos, T. and Bédard, C. (2006), "Effect of upstream hills on design wind load: a computational approach", *Wind Struct*., **9**(1), 37-58.

Chang, C.C. (1971), "Tornado effects on building and structures with laboratory simulation", *Proceedings of the 3rd Int. Conf. on Wind Effects on Buildings and Structures*, Saikon, Tokyo.

Church, C., Burgess, D., Doswell, C. and Davies-Jones, R. (1993), Tornado: Its structure, dynamics, predictions and hazards. Washington, D.C., USA, American Geophysical union.

Davies-Jones, R.P. (1973), "The dependence of core radius on swirl ratio in a tornado simulator", *J. Atmos. Sci*., **30**, 1427-1430.

Diamond, C.J. and Wilkins, E.M. (1984), "Translation effects on simulated tornadoes", *J. Atmos. Sci*., **41**, 2574-2580.

Forbes, G.S. (1998), "Topographic influences on tornadoes in Pennsylvania", Preprints, *Proceedings of the 19th Conference on Severe Local Storms*, Amer. Meteor. Soc., Minneapolis, MN.

Fouts, L., James, D.L. and Letchford, C.W. (2003), "Pressure distribution on a cubical modeling tornado-like flow", *Proceedings of the 10th Intl Wind Engineering Conf*., Texas, Tech. Univ., Lubbock, Texas.

Francis, H.H. and Leland, R.S. (1974), "Structural analysis of tornado-like vortices", *J. Atmos. Sci*., **31**, 2081-2091.

Giaiotti, D.B. and Stel, F. (2005), The Rankine vortex model (Doctoral thesis). University of Trieste, Italy.

Haan Jr, F.L., Balaramudu, V.K. and Sarkar, P.P. (2010), "Tornado induced wind loads on a low-rise building", *J. Struct. Eng*., **136**, 106-116.

Haan, F.L., Jr., Sarkar, P.P. and Gallus, W.A. (2008), "Design, construction and performance of a large tornado simulator for wind engineering applications", *Eng. Struct*., **30**, 1146-1159.

Hamada, A. and El Damatty, A.A. (2011), "Behaviour of guyed transmission line structures under tornado wind loading", *J. Comput. Fluid Solid Mech*., **89**(11-12), 986-1003.

Hangan, H. and Kim, J.D. (2008), "Swirl ratio effects on tornado vortices in relation to the Fujita scale", *Wind Struct*., 11(4), 291-302.

Hashemi-Tari, P., Gurka, R. and Hangan, H. (2010), "Experimental investigation of tornado-like vortex dynamics with Swirl Ratio: The mean and turbulent flow fields", *J. Wind Eng. Ind. Aerod*., **98**.

Ishac, M.F. and White, H.B. (1994), "Effect of tornado loads on transmission lines", *Proceedings 528 of the 1994 IEEE Power Engineering Society Transmission and Distribution Conference*, 10-15, 529 April 1994, IEEE, Chicago, IL, USA.

Ishihara, T, Oh, S. and Tokuyama, Y. (2011), "Numerical study on flow fields of tornado-like vortices using the LES turbulence model", *J. Wind Eng. Ind. Aerod*., **99**, 239-248

Jischke, M.C. and Light, B.D. (1983), "Laboratory simulation of tornadic wind loads on a rectangular building", *J. Wind. Eng. Ind. Aerod*., **13**(1-3), 274-282.

Karstens, C.D. (2012), Observations and Laboratory Simulations of Tornadoes in Complex Topographical Regions, PhD Dissertation, Department of Meteorology, Iowa State University.

Kuai, L., Haan, Jr. F.L., Gallus, Jr. W.A., and Sarkar, P.P. (2008), "CFD simulations of the flow field of a laboratory-simulated tornado for parameter sensitivity studies and comparison with field measurements", *Wind Struct*., **11**(2), 75-96.

Launder, B.E., Reece, G.J. and Rodi, W. (1975), "Progress in the development of a Reynolds-stress turbulence closure", *J. Fluid Mech.*, **68**(3), 537-566.

Lewellen, D.C. (2012), "Effects of topography on tornado dynamics", *Proceedings of the 26th Conference on Severe Local Storms*, November 5-8, Nashville, TN, USA.

Lewellen, D.C. and Lewellen, W.S. (1997), "Large eddy simulation of tornado's interaction with the surface", *J. Atmos. Sci*., **54**(5), 581-605.

Lewellen, D.C. and Lewellen, W.S. (2007), "Near-surface intensification of tornado vortices", *J. Atmos. Sci*., **64**, 2176-2194.

Lun, Y.F., Mochida, A., Yoshino, H., Murakami, S. and Kimura, A. (2003), "Applicability of linear type revised k−ε models to flow over topographic feature", *Proceedings of the 11th International Conference on Wind Engineering*, June 2-5, Lubbock, Texas, USA.

Matsui, M. and Tamura, Y. (2009), Influence of swirl ratio and incident flow conditions on generation of tornado-like vortex. EACWE 5.

Maurizi, A. (2000), "Numerical simulation of turbulent flows over 2D valleys using three versions of the k−ε closure model", *J. Wind Eng. Ind. Aerod*., **85**, 59-73.

McCarthy, P. and Melsness, M. (1996), Severe weather elements associated with September 5, 1996 hydro tower failures near Grosse Isle, Manitoba, Canada, Manitoba Environmental Service Centre, Environment Canada.

Mehta, K.C., McDonald, J.R. and Minor, J.R. (1976), Wind speeds Analyses of April 3-4, 1974 Tornadoes. American Society of Civil Engr. 102-9, 1709-1724.

Mishra, A.R., James, D.L. and Lecthcford, C.W. (2003), "Comparison of pressure distribution on a cubical model in boundary layer and tornado-like flow fields", *Proceedings of the Americas Conference on Wind Engineering*, Baton Rouge, LA, USA.

Mitsuta, Y. and Monji, N. (1984), "Development of a laboratory simulator for small scale atmospheric vortices", *Natural*

Disaster Science, **6**, 43-54.
Nasir, Z. and Bitsuamlak, G.T. (2014), "Similarities and differences among tornadic and synoptic flow induced loads on a building", *Proceedings of the Engineering Mechanics Institute Conference*, Hamilton, ON, Canada.
Nasir, Z., Bitsuamlak, G.T. and Hangan, H. (2014), "Computational modeling of tornadic load on a building", *Proceedings of the 6th International Symposium on Computational Wind Engineering*, Hamburg, Germany, June 8-12, 2014.
Natarajan, D. and Hangan, H. (2012), "Large eddy simulation of translation and surface roughness effects on tornado-like vortices", *J. Wind Eng. Ind. Aerod.*, **104-106**, 577-584.
Nolan, D.S. and Ferrell, B.F. (1999), "The structure and dynamics of tornado-like vortices", *J. Atmos. Sci.*, **56**, 2908-2936.
Refan, M., Hangan, H. and Wurman, J. (2013), "Reproducing tornadoes in laboratory using proper scaling", *Proceedings of the 12th Americas Conference on Wind Engineering*, June 16-20, 2013, Seattle, Washington.
Rotunno, R. (1977), "Numerical simulation of a tornado vortex", *J. Atmos. Sci*., **34**, 1942-1956.
Rotunno, R. (1979), "A study in tornado-like vortex dynamics", *J. Atmos. Sci*., **36**, 140-156.
Sarkar, P.P., Haan, F.L., Balaramudu, V. and Sengupta, A. (2006), "Laboratory simulation of tornado and microburst to assess wind loads on buildings", *Proceedings of the ASCE Structures Congress*, ASCE, Reston, Va.
Selvam, R.P. and Millet, P.C. (2003), "Computer modeling of tornado forces on a cubic building using large eddy simulation", *Arkansas Academy of Sci*., **57**, 140-146.
Sengupta, A., Haan, F.L., Sarkar, P.P. and Balaramudu, S.V. (2006), "Transient loads on buildings in microburst and tornado winds", *Proceedings of the 4th International Symposium on Comp. Wind Engr. (CWE2006)*, Yokohama, Japan.
Wang, H., Letchford, J.D. and Snow, R.J. (2001), "Development of a prototype tornado simulator for the assessment of fluid-structure interaction", *Proceedings of the 1stAmericas Conference in Wind Engineering*, Clemson, SC.
Ward, N.B. (1972), "The exploration of certain features of tornado dynamics using a laboratory model", *J. Atmos. Sci*., **29**, 1194-1204.
Zhang, W. and Sarkar, P.P. (2012), "Near-ground tornado-like vortex structure resolved by particle (PIV)", *Exp. Fluids*, **52**(2), 479-493.